we expect to describe the temperature dependence of the photochemistry of this compound shortly.

Acknowledgment. Support for this work was provided by the CNRS, the Texas Advanced Research Program, and the National Science Foundation (CHE 9102657). The CFKR is supported jointly by the Division of Research Resources of the NIH (RR00886) and by The University of Texas at Austin. We thank the U.S. Department of Energy for the award of a grant enabling construction of the subpicosecond laser flash spectrometer.

Controlling Solid-State Reaction Mechanisms Using Diffusion Length in Ultrathin-Film Superlattice Composites

Loreli Fister and David C. Johnson*

Contribution from the Department of Chemistry and Materials Science Institute, University of Oregon, Eugene, Oregon 97403. *Received October 21, 1991*

Abstract: The synthetic parameters used by solid-state chemists have essentially been limited to temperature, pressure, composition, and time. Diffusion length can also be used as a synthetic parameter to alter the pathway of a solid-state reaction. Modulated, binary, ultrathin films of similar stoichiometry have been made whose repeat distance varies from 18 to 128 Å. For samples whose modulation length is 38 Å or larger, the films evolve upon heating as thin-film diffusion couples, initially growing an amorphous layer and then crystallizing a stable product, $MoSe_2$, at the interface between individual elemental layers. For samples of 27 Å or smaller, the films evolve to a homogeneous, amorphous alloy before crystallizing $MoSe_2$. This implies a critical layer thickness, below which it is possible to form a homogeneous, amorphous alloy. There is a difference in nucleation temperature of several hundred degrees between the two length scales reflecting the importance of interfaces in aiding nucleation. The synthetic importance of these results—the ability to control synthetic variables to reach desired reaction intermediates in solid-state reactions—is highlighted.

Introduction

Molecular chemistry is based upon the kinetic control of the reaction pathway to obtain kinetic products. *In contrast, this general ability to control the reaction pathway does not exist in solid-state synthesis.* Traditional solid-state synthetic techniques involve large diffusion distances in the initial reactants. Classic studies of bulk diffusion couples have shown that the growth of crystalline products rapidly becomes limited by the diffusion of the reactants through the product layer.[1] In this diffusion-limited regime, all stable phases found in the equilibrium phase diagram are formed as intermediates on the way to the final products. An example of this reaction is shown in Figure 1 for a molybdenum–selenium diffusion couple. The amount of each phase is determined by the relative diffusion rates of each atom through the various intermediate compounds.[2] A consequence of this bulk diffusion couple reaction is that only the most thermodynamically stable final products can be produced.

In contrast to bulk diffusion couples, kinetic evolution has been observed in diffusion couples, made by the sequential deposition of the reacting elements, whose layer thicknesses were several hundred angstroms.[1,3-8] As these diffusion couples are heated, a compound is observed to nucleate at the interface and grow until its growth exhausts one of the reactants.[9] Only then is another crystalline phase observed to nucleate at the compound–element interface.[10] The new compound grows until it exhausts either the supply of compound or element. This process repeats until the equilibrium mix of products is obtained. The sequence of phases formed on the way to this state depends upon the relative activation energies for nucleation of the various compounds. Compounds in the equilibrium phase diagram may be temporarily skipped if they have a large activation energy for nucleation. This reaction pathway is alternately limited by diffusion and nucleation, as illustrated in Figure 2.

There is a maximum thickness of the elemental layers which separates the above behavior from that observed in a bulk diffusion couple. This maximum thickness depends upon the rate of diffusion through the growing product layer and the activation energy necessary to nucleate a product at either of the compound–element interfaces. This behavior has been extensively investigated in metal–metal and metal–metalloid systems and the term "thin-film diffusion couple" has been coined to describe this thickness regime.

Although studies of thin-film diffusion couples have demonstrated a different and kinetically-controlled reaction mechanism, thin-film diffusion couples still do not permit control of the reaction intermediates. Conceptually, a solid-state reaction can be broken into two key steps: the interdiffusion of the reactants and the nucleation/crystallization of products. Thin-film diffusion couples are alternately limited by diffusion and nucleation. Any attempt to gain complete, kinetic control of the reaction pathway must be based upon eliminating diffusion as a rate-limiting step. This leaves nucleation, a kinetic phenomenon dependent upon overcoming a reaction barrier, as the crucial step to control.

A homogeneous, amorphous alloy is an ideal reaction intermediate for the preparation of extended solids. Long-range diffusion is completed in the formation of the alloy. This leaves nucleation as the rate-limiting step in the formation of a crystalline solid. Nucleation can be controlled by several strategies including impurities acting as nucleation seeds, using crystalline substrates

* Author to whom correspondence should be addressed.

(1) Gösele, U.; Tu, K. N. *J. Appl. Phys.* **1989**, *66*, 2619–2626.
(2) Brophy, J. H.; Rose, R. M.; Wulff, J. In *Thermodynamics of Structure*; John Wiley & Sons: New York, 1964; pp 91–94.
(3) Herd, S.; Tu, K. N.; Ahn, K. Y. *Appl. Phys. Lett.* **1983**, *42*, 597–599.
(4) Nava, F.; Psaras, P. A.; Takai, H.; Tu, K. N. *J. Appl. Phys.* **1986**, *59*, 2429–2438.
(5) Gas, P.; d'Heurle, F. M.; LeGoues, F. K.; La Placa, S. J. *J. Appl. Phys.* **1986**, *59*, 3458–3466.
(6) Coulman, B.; Chen, H. *J. Appl. Phys.* **1986**, *59*, 3467–3474.
(7) Clemens, B. M.; Buchholz, J. C. *Mater. Res. Soc. Symp. Proc.* **1985**, *37*, 559–564.
(8) Desré, P. J.; Yavari, A. R. *Phys. Rev. Lett.* **1990**, *64*, 1533–1536.
(9) Walser, R. M.; Benê, R. W. *Appl. Phys. Lett.* **1976**, *28*, 624–625.
(10) Tsaur, B. Y.; Lau, S. S.; Mayer, J. W.; Nicolet, M.-A. *Appl. Phys. Lett.* **1981**, *38*, 922–924.

0002-7863/92/1514-4639$03.00/0

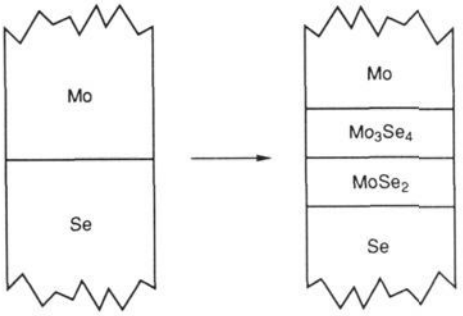

Figure 1. Schematic of a partially reacted bulk diffusion couple of molybdenum and selenium.

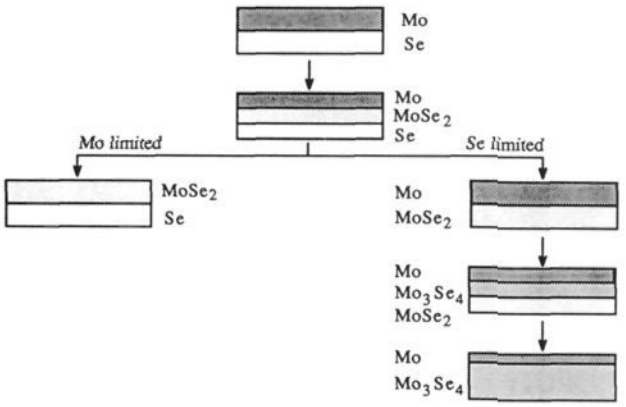

Figure 2. Schematic of the evolution of a "thin-film diffusion couple" of molybdenum and selenium.

as templates for nucleation, and through such basic chemical parameters as composition of the alloy. The use of this reaction intermediate in systems other than metal–metal and metal–metalloid alloys has been limited by the ability to isolate bulk amorphous material.

Routes to amorphous alloys described in the literature include the rapid cooling of molten alloys commonly referred to as splat cooling or melt spinning, the codeposition of the respective elements, and the low-temperature interdiffusion of superlattice composites. There are several drawbacks to each of these techniques for the preparation of amorphous alloys as synthetic reaction intermediates. Amorphous phase formation by rapid quenching of a high-temperature liquid is complicated by the importance of experimental variables such as quench rates on the structure of the product. Rapid quenching is also limited to systems in which it is possible to form homogeneous melts. The properties of the amorphous alloys produced by codeposition are influenced by the rate of deposition and the temperature of the substrate. The low-temperature interdiffusion route has been limited to cases involving anomalously rapid diffusion by one of the elements in the system. All of these techniques as reported in the literature are also limited in the stoichiometries that can be prepared.[11] Investigations have generally been limited to metal–metal and metal–metalloid systems.

An important reaction parameter, the thickness of the layers, has not been previously explored in the low-temperature interdiffusion of superlattice composites. The typical length scales of solid-state amorphization reactions presented in the literature have been hundreds of angstroms. The thickness of the reacting layers affects two of the important parameters limiting the formation of amorphous alloys: the time necessary to interdiffuse the layers and the temperature required for this interdiffusion. The time necessary to interdiffuse a superlattice can be obtained from Fick's laws of diffusion. This time is proportional to the square of the diffusion distance. The temperature required for diffusion depends upon the local structure within the multilayer. This dependence

(11) Saunders, N.; Miodownik, A. P. *J. Mater. Res.* **1986**, *1*, 38–46.

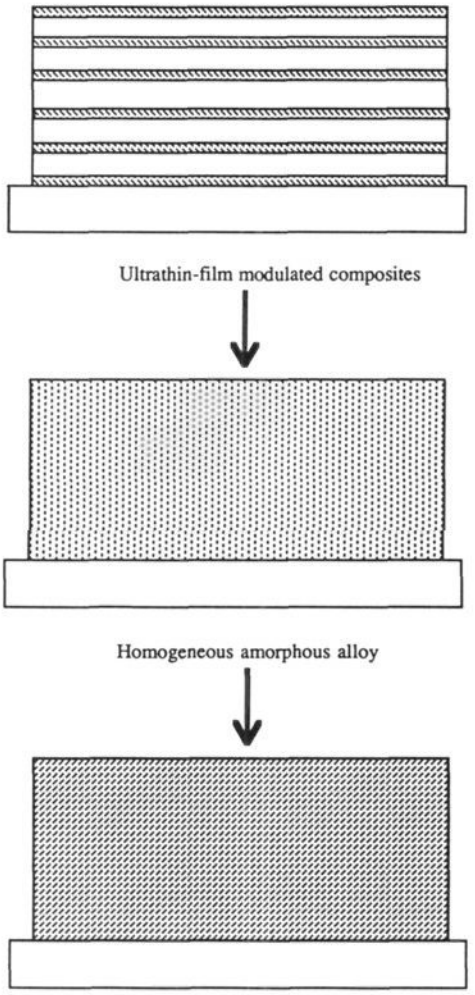

Figure 3. Reaction mechanism for ultrathin-film composites showing the formation of a homogeneous, amorphous alloy as the key reaction step.

is seen experimentally as the diffusion rate decreases with reaction time as high-energy conformations are eliminated.[12]

We decided that low-temperature interdiffusion of superlattice composites, modulated on an angstrom or tens of angstrom length scale, was the best option available for preparing amorphous alloys because it is the most diffusionally constrained. Herein, we present the results of our investigation into the effect of length scale upon the course of a solid-state reaction. This study is based upon the idea that both diffusion and nucleation are competing in the reaction of two solids. By reducing the layer thicknesses, we increase the probability diffusion will be completed before nucleation of a product occurs.

The use of ultrathin superlattice composites as initial reactants provides other benefits as well. The structure of the initial composite, the layering sequence, and layer thicknesses can be tailored to facilitate the desired reaction pathway, shown in Figure 3. In this pathway the reactants initially diffuse without nucleating a crystalline compound, forming instead a homogeneous, amorphous alloy. This alloy then crystallizes directly to the desired crystalline compound. The rate-limiting step in this proposed reaction mechanism is nucleation.[13]

Little is known about the earliest stages of solid-state reactions—i.e. before the formation of a crystalline product at the interface.[14] The interfaces of a bulk diffusion couple make

(12) Novet, T.; McConnell, J. M.; Johnson, D. C. *J. Mater. Chem.* **1992**, *4*, 473–478.
(13) Novet, T.; Johnson, D. C. *J. Am. Chem. Soc.* **1991**, *113*, 3398–3403.

up only a minute fraction of the sample and such buried interfaces are difficult to observe. Superlattice reactants can be modulated on a fine enough length scale such that they consist almost entirely of interfaces. The diffraction pattern resulting from the modulated structure of a superlattice contains information about the structure of the interfaces. The decay of this diffraction pattern as the films interdiffuse permits the evolution of the interfaces to be followed.[12,15,16]

The molybdenum–selenium system was selected to study the effect of layer thickness upon the solid-state reaction pathway. Our objective was to reduce the layer thicknesses within the composite to form, upon interdiffusion, a homogeneous, amorphous alloy of molybdenum and selenium before the nucleation of $MoSe_2$. A previous investigation[17] and our own preliminary studies indicated that $MoSe_2$ crystallizes at very low temperatures (~200 °C). The low nucleation temperature for molybdenum diselenide is a consequence of its small crystallographic unit cell, its two-dimensional structure with directional, covalent bonding, and its large heat of formation from the elements. In addition, molybdenum–selenium compounds decompose to molybdenum metal and selenium vapor at temperatures above 1400 °C. This combination of properties, inherent to the system, makes the formation of an amorphous molybdenum–selenium alloy exceedingly difficult. Preparation of an amorphous alloy in this system via a solid-state interdiffusion reaction represented a significant synthetic challenge.

Experimental Section

Sample Preparation. A custom-built ultra-high-vacuum (UHV) chamber with independently controlled electron beam and effusion deposition sources was used to prepare the multilayer films used in this study. Complete details of this chamber can be found elsewhere.[18] Molybdenum was deposited at a rate of 0.5 Å/s using an electron beam source controlled by quartz crystal monitors. Selenium was deposited from a Knudsen source maintained at a temperature of 235 °C, resulting in a deposition rate of approximately 1.2 Å/s. Silicon wafers polished to ±3 Å rms were used as substrates for the multilayer composites produced.

X-ray Diffraction. The modulation thicknesses and interfacial widths were determined from the low-angle diffraction data of the multilayer composites. The diffraction data were collected on a Scintag XDS 2000 θ–θ diffractometer on which the sample stage had been modified to allow rapid and precise alignment. Low-angle diffraction data were used to confirm the layered nature of the starting composites, determine the layer spacing, and get an estimate of the interfacial width. High-angle diffraction data were used to determine whether the film contained crystalline elements or compounds.

Differential Scanning Calorimetry. Differential scanning calorimetry (DSC) was used to assess the reaction between the elemental layers in a composite quickly and quantitatively as a function of temperature.[19] The DSC experiment required approximately 1 mg of layered composite free of the substrate. These samples were obtained by first coating a silicon wafer with poly(methyl methacrylate) (PMMA) using a 3% PMMA in chlorobenzene solution and a spincoater rotating at 1000 rpm. The desired multilayer structure was then deposited upon the coated wafer. After the sample was removed from the deposition chamber, it was immersed in acetone, which dissolved the PMMA and floated the multilayer film off the substrate. The resulting small pieces were collected via sedimentation into an aluminum DSC pan. The sample was dried under reduced pressure to remove residual acetone and the pan was crimped closed.

The sample was then placed in a TA Systems 910 DSC module with an empty pan as the reference container. The DSC module was contained within a nitrogen atmosphere drylab (0.5 ppm of oxygen) to prevent oxidation of the sample during heating. The samples were heated at 10 °C/min from room temperature to 600 °C. After they had cooled to room temperature, the samples were reheated to obtain a baseline for the irreversible changes which occurred during the initial heating. Typically, a second such background was collected to obtain a measure of the repeatability of the experiment. The net heat absorbed or released from the multilayer sample as diffusion occurred was obtained from the difference between the first DSC experiment and the subsequent runs. The two background runs were within 0.05 mW/mg, indicating the degree of repeatability of the experiments.

High-Temperature X-ray Diffraction. High-temperature X-ray diffraction data were collected as a function of temperature and time on two samples to determine the cause of the exotherms found in the differential scanning calorimetry experiments. The sample was placed in a specially designed high-temperature/controlled-atmosphere X-ray chamber which was then evacuated to 8×10^{-7} Torr. A reference low-angle pattern was then taken (0.2–7°, 2θ), along with a high-angle pattern (2–80°, 2θ). The sample was then heated to approximately 110 °C. A low-angle pattern was taken and compared against the room temperature reference pattern to check the alignment of the diffractometer. Once the diffractometer alignment was verified, low-angle diffraction scans were taken at 10-min intervals for several hours. At the end of this time, another high-angle diffraction pattern was taken. Additional high-temperature experiments were run by simply increasing the heat to the new desired temperature, verifying the alignment, and then running the low-angle diffraction scans. At the end of the low-angle scans another high-angle X-ray pattern was taken to check the crystallinity of the sample.

Table I. Summary Table of the Samples Prepared as Part of This Investigation[a]

intended thickness			meas	no. of
Mo	Se	total	total	layers
6	14	20	18	35
9	21	30	27	6
9	21	30	26	40
12	28	40	38	18
12	28	40	n/a	39
15	35	50	54	30
18	42	60	62	26
22	52	74	60	30
30	70	100	80	30
38	87	125	92	19
45	105	150	128	22

[a] All lengths are measured in Å.

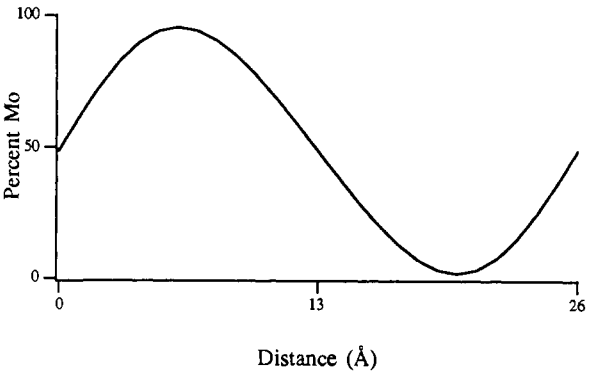

Figure 4. A schematic illustration of composition as a function of distance within a 26-Å repeat unit of a molybdenum–selenium superlattice.

Results

A series of molybdenum–selenium samples of the same composition but varying modulation length were prepared. Table I contains a summary of the multilayer composites prepared for this study, giving the layer thicknesses both intended and actual as determined from the low-angle diffraction data. The positions of the Bragg diffraction peaks, corrected for the change in the index of refraction at the sample surface, were used to determine the size of the repeat unit in the multilayer composite being examined. The initial high-angle X-ray scans suggest that the elemental layers in these films were amorphous rather than crystalline as deposited.

The low-angle diffraction patterns contain much information about film structure. The rate of the intensity decrease of the background and the angle at which the subsidiary maxima between

(14) Mayer, J. W.; Poate, J. M.; Tu, K.-N. *Science* **1975**, *190*, 228–234.
(15) Prokes, S. M.; Spaepen, F. *Appl. Phys. Lett.* **1985**, *47*, 234–236.
(16) Fleming, R. M.; McWhan, D. B.; Gossard, A. C.; Wiegmann, W.; Logan, R. A. *J. Appl. Phys.* **1980**, *51*, 357–363.
(17) Jäger-Waldau, A.; Lux-Steiner, M.; Jäger-Waldau, R.; Burkhardt, R.; Bucher, E. *Thin Solid Films* **1990**, *189*, 339–345.
(18) Fister, L.; Li, X. M.; Novet, T.; McConnell, J.; Johnson, D. C., in **preparation**.
(19) Cotts, E. J.; Meng, W. J.; Johnson, W. L. *Phys. Rev. Lett.* **1986**, *57*, 2295–2298.

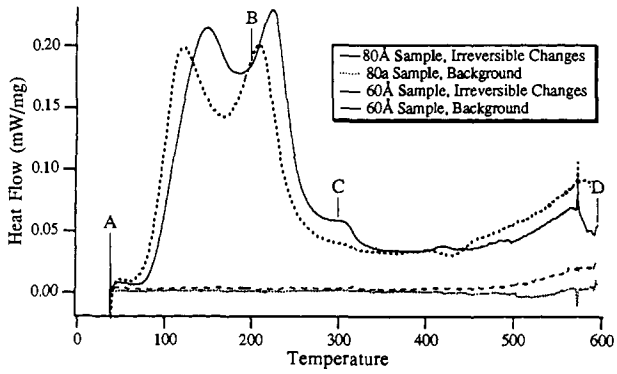

Figure 5. Differential scanning calorimetry data for the reaction of superlattices of molybdenum and selenium with repeat units of 60 and 80 Å, respectively.

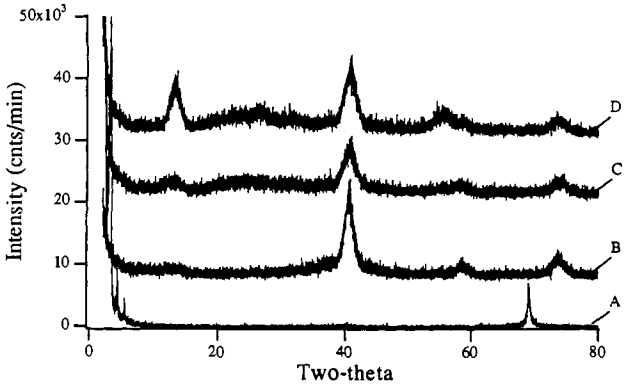

Figure 6. Diffraction data collected during of reaction of the molybdenum–selenium composite with a repeat distance of 80 Å: (A) at room temperature, (B) at 200 °C, (C) at 300 °C, and (D) at 600 °C. Data sets are offset vertically for clarity. The diffraction peaks observed in scans B–D are the 00ℓ lines of $MoSe_2$ indicating a preferred orientation of the product. The peak at ~72° on diffraction pattern A is due to the silicon wafer substrate.

the Bragg diffraction peaks are no longer observed was used to estimate the coherence of the layers within the composite.[12,20-24] For the samples discussed in this paper, the composites are coherent to within approximately ±3 Å. The relative intensity of the peaks can be compared with that calculated for a sample with abrupt interfaces to give an indication of the average sharpness of the interface between elemental layers in these films.[16] For the samples discussed in this paper, the interfacial widths are all approximately 15 ± 5 Å as illustrated schematically in Figure 4. Thus the amorphous nature of the initial layered elements is a result of the significant interdiffusion between the elemental layers during deposition. This interdiffusion inhibits the crystallization of the deposited elements.

Differential scanning calorimetry was used to investigate the reaction pathway of the multilayer composites. Figure 5 shows the heat evolution as a function of temperature for the composites with layer spacings of 60 and 80 Å, respectively. This graph is representative of all of the samples with a layer spacing of 38 Å and larger. Each of these data sets contains two overlapping exotherms below 250 °C. Diffraction data collected on the 80-Å sample heated to the points A, B, C, and D indicated in Figure 5 are shown in Figure 6. These data demonstrate that by the beginning of the second exotherm $MoSe_2$ has nucleated.

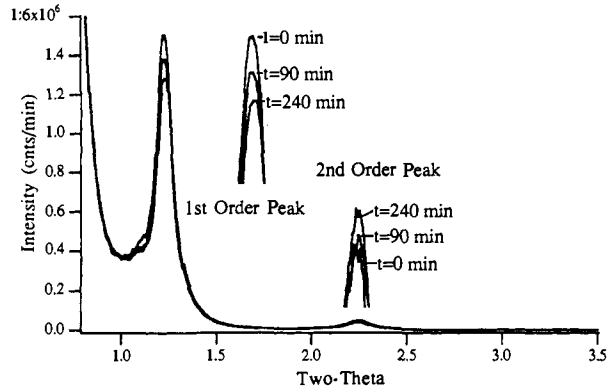

Figure 7. Low-angle diffraction patterns of an 80-Å sample at times 0, 90, and 240 min while being annealed at 184 °C.

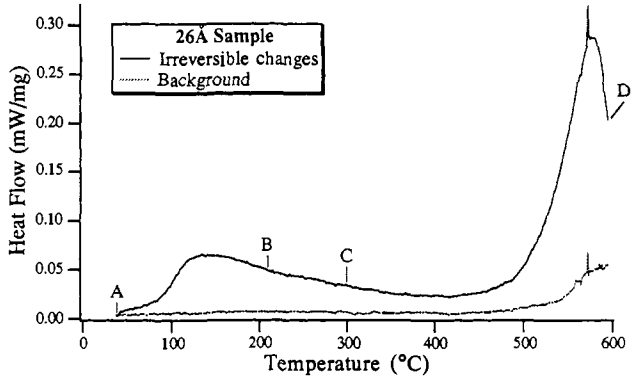

Figure 8. Differential scanning calorimetry data for the 26-Å modulation length sample.

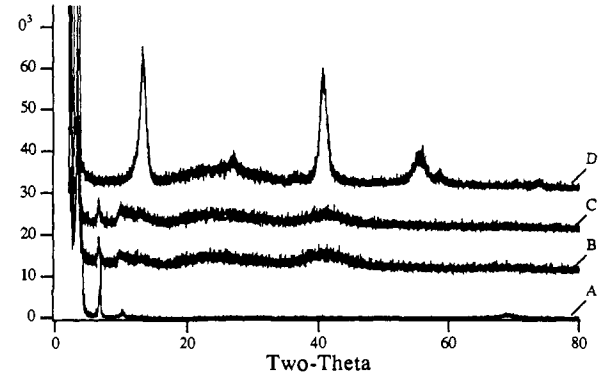

Figure 9. Diffraction data collected during the reaction of the 26-Å sample: (A) at room temperature, (B) at 200 °C, (C) at 300 °C, and (D) at 600 °C. Data sets are offset vertically for clarity. The broad maxima at approximately 24° in B–D are from the glass substrate. The diffraction peaks in D are the 00ℓ diffraction lines of $MoSe_2$. The phase grows with a preferred orientation.

Low- and high-angle diffraction data collected on the 80-Å sample as a function of temperature from 100 to 184 °C support the conclusion that the first exotherm is due to the initial interdiffusion of the layers. Any change in the intensity of the Bragg diffraction peak with temperature and time can be used to follow the interdiffusion process.[12,25] The intensity of the X-ray diffraction peaks is related to the coefficient of a Fourier expansion of the electron density within a repeat unit of the composite.[26] If a smooth composition gradient exists between elements, all the diffraction peaks should decrease with time and have the same diffusion constant. The first-order peak is seen to decrease as expected, but the second-order diffraction peak grows with time,

(20) Nêvot, L.; Pardo, B.; Corno, J. *Rev. Phys. Appl.* **1988**, *23*, 1675–1686.
(21) Savage, D. E.; Kleiner, J.; Schimke, N.; Phang, Y.-H.; Jankowski, T.; Jacobs, J.; Kariotis, R.; Lagally, M. G. *J. Appl. Phys.* **1991**, *69*, 1411–1424.
(22) Spiller, E. *Rev. Phys. Appl.* **1988**, *23*, 1687–1700.
(23) Falco, C. M.; Fernandez, F. E.; Dhez, P.; Khander, A.; Nevot, L.; Pardo, B.; Corno, J. *Proc. SPIE* **1987**.
(24) Falco, C. M. In *Growth of Metallic and Metal-Containing Superlattices*; Dhez, P., Weisbuch, C., Eds.; Plenum Press: New York, 1988; pp 3–15.
(25) Greer, A. L.; Spaepen, F. In *Diffusion*; Chang, L. C., Giessen, B. C., Eds.; Academic Press: New York, 1988; pp 419–486.
(26) DuMond, J.; Youtz, J. P. *J. Appl. Phys.* **1940**, *11*, 357–365.

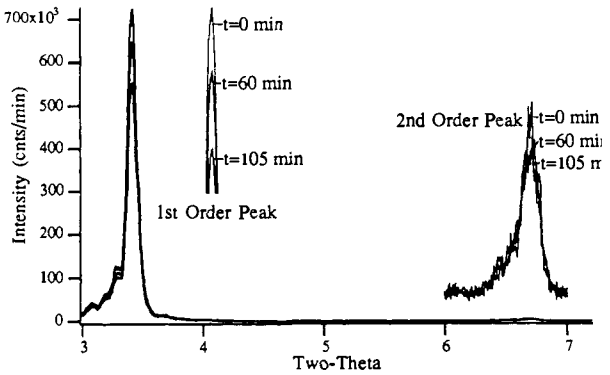

Figure 10. Intensities of low-angle diffraction data of the 26-Å sample taken at time 0, 60, and 105 min while being annealed at 222 °C.

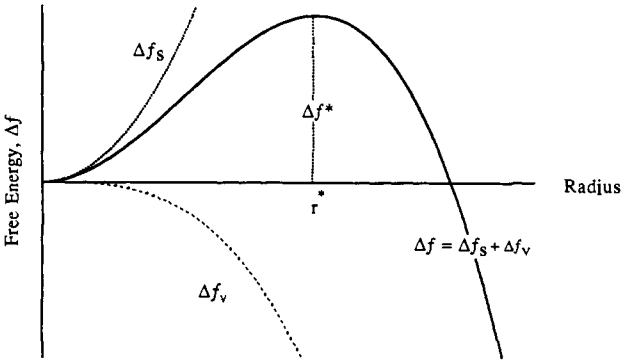

Figure 11. The radial dependence of the free energy for homogeneous nucleation of spherical nuclei from a homogeneous liquid.

as seen in Figure 7. This indicates that a plateau of composition develops in the interface region as the amorphous interface expands. Once this plateau reaches a critical size, $MoSe_2$ is observed to nucleate and grow, resulting in the second exotherm. This behavior agrees with the generally accepted picture for the solid-state reaction between two elements. Thus, a layered Mo–Se composite with a repeat unit of approximately 38 Å or greater behaves as if each interface were a thin-film diffusion couple.

The behavior observed for composites of 27 Å or less in modulation length is distinctly different than that described above for composites with thicker modulation distances. This is illustrated by the differential scanning calorimetry data for a sample with a 26-Å repeat unit, shown in Figure 8. The samples with a layer spacing of less than 26 Å show a broad maximum beginning at 100 °C followed by a large exotherm with a maximum at 575 °C. Figure 9 shows diffraction data collected on samples heated to points A, B, C, and D in Figure 8. The broad maxima at approximately 41° in patterns B and C are due to the distribution of molybdenum–selenium bond distances within the amorphous alloy. Extended heating of the sample at 350 °C for 26 h completely eliminated the low-angle diffraction peaks while the intensity and line width of the broad maxima at 41° were not affected by this heating. Crystalline $MoSe_2$ is observed only after the large exotherm at 575 °C.

Low-angle diffraction data collected as a function of temperature from 109 to 222 °C confirm that the first exotherm is due to the initial interdiffusion of the layers. The intensities of the low-angle diffraction peaks are plotted in Figure 10. Compared with the 80-Å composite discussed earlier, the plateau growth is severely depressed as indicated by the decay of the second-order diffraction peak with time. High-angle diffraction scans indicate that the sample remains amorphous as the sample completely interdiffuses.

Discussion

We have modified the reaction path of a solid-state reaction by adjusting the layer thickness of the initial composite. In the ultrathin-film regime the interfaces disappear quickly due to the short length scale for diffusion, supporting the reaction mechanism depicted in Figure 3. The composite interdiffuses completely forming a homogeneous, amorphous alloy before any binary phase nucleates. This is distinctly different than what is observed in composites layered with a larger repeat distance. Above a critical layer thickness the composites behave as thin-film diffusion couples with nucleation occurring at the interfaces.

There is a surprisingly large difference in the nucleation temperatures for composites in these two different length-scale regimes. This large difference can be understood by considering the factors affecting nucleation within a solid matrix.[27] The transformation of a metastable, amorphous intermediate into a thermodynamically more stable crystalline product initially begins on a very small scale due to entropy considerations. This nucleation step involves the assemblage of the proper kinds of atoms via diffusion, structural rearrangement into intermediates, and the formation of stable nuclei.[28]

Nucleation from a homogeneous fluid system provides a simple model for understanding our observed changes in nucleation temperature with modulation length. Suppose a small region of a stable crystalline compound, referred to as an embryo, appears in the middle of a melt with stoichiometry identical to that of the crystalline compound. A free energy decrease per unit volume, Δf_v, would be expected as a result of the conversion of the metastable liquid to the crystalline compound. This embryo is bounded by a surface which has a positive free energy per unit area, Δf_s, associated with it. If the embryo grows above a "critical" radial size (r^*), Δf_v dominates and the embryo survives to nucleate, otherwise Δf_s dominates and the embryo disappears back into the melt as shown pictorially in Figure 11.[29]

In the longer length-scale regime, nucleation occurs in the concentration gradient at the interface. The composition gradients enhance diffusion rates and the interface region has large stresses and strains resulting from differences in the mechanical properties of the elements. These effects combine to lower the surface energy component, Δf_s, for nucleation at interfaces, making nucleation easier in this region. This picture explains why crystalline compounds are observed to nucleate preferentially at interfaces and surfaces[29,30] and agrees with our own observations that nucleation occurs at lower temperatures in the longer length-scale regime.

In the case of ultrathin films, nucleation occurs after diffusion is complete. Since all of the interfaces have diffused away, nucleation of a binary phase is more difficult due to the disappearance of the stresses and strains inherent in interfacial regions. This is more like the case of homogeneous nucleation, shown in Figure 11. Due to the larger Δf^*, nucleation is delayed by several hundred degrees in the thin-film cases compared with the thick-film case.

The large difference in nucleation temperatures in the two different length-scale regimes increases the synthetic importance of the ultrathin-film reaction mechanism. The amorphous Mo–Se alloy formed from the ultrathin-film composites is surprisingly stable. The crystalline compound which forms from this homogeneous alloy depends only on the relative barriers to nucleation for the possible compounds, not on their final free energy states.

The proposed mechanism, shown in Figure 3, for ultrathin-film reactions allows us rationally to design a synthetic sequence to a desired product. This ability is especially important for ternary and other higher-order compounds. Traditional synthetic approaches involve stable binary compounds as reaction intermediates. These approaches are therefore limited to finding a region of phase space in which the desired compound is thermodynamically the most stable one.[31]

Our results suggest a set of sequential steps aimed at controlling the evolution of a superlattice to a homogeneous, amorphous

(27) Cahn, J. W.; Hilliard, J. E. *J. Chem. Phys.* **1959**, *31*, 688–699.

(28) Gibbs, J. W. *Collected Works*; Yale University Press: New Haven, CT, 1948; pp 105–115, 252–258.

(29) Brophy, J. H.; Rose, R. M.; Wulff, J. In *Thermodynamics of Structure*; John Wiley & Sons: New York, 1964; pp 98–108.

(30) Calka, A.; Radlinski, A. P. *Acta Metall.* **1987**, *35*, 1823–1829.

(31) DiSalvo, F. J. *Science* **1990**, *247*, 649–655.

reaction intermediate. The design sequence starts with determining the critical diffusion distances in the binary diffusion couples. A ternary composite is then prepared such that all of the diffusion distances are subcritical, the layer sequence is chosen so as to control the interdiffusion process,[32] and the stoichiometry is selected to be that of the desired ternary compound. Upon heating, this composite should form a homogeneous, ternary, amorphous alloy.[33]

The key to obtaining the desired compound is controlling the nucleation of this amorphous alloy. There are several approaches which can be used to achieve this goal. Stoichiometry has been shown to control the phase which nucleates from the amorphous alloy.[13] Since the amorphous alloy contains three elements, nucleation of binary compounds should be suppressed and should favor the nucleation of ternary compounds. Additional experimental variables which can be used to influence nucleation temperatures include the crystal structure of the substrate surface[34] and the addition of controlled impurities acting as nucleation agents.[35] This synthetic sequence, separating the mixing of the elemental reactants from nucleation of crystalline compounds, should permit the synthesis of ternary compounds which are unstable with respect to competing binary phases. Work toward this goal is in progress.

Conclusion

We have shown that the course of a solid-state reaction can be controlled by varying the length scale of the initial composite. A mechanism for the solid-state reaction of ultrathin films is presented. The synthetic importance of using diffusion distances to control the intermediates of the solid-state reaction is emphasized. Further work based upon the proposed mechanism is focused upon directly nucleating ternary compounds from amorphous precursors and controlling nucleation and the synthesis of single-crystal thin films from the homogeneous, amorphous alloy intermediate.

Acknowledgment. We acknowledge the assistance of T. Novet, J. McConnell, and C. Grant for helpful discussions and advice. This work was supported in part by a Young Investigator Award from the Office of Naval Research (No. N0014-87-K-0543). Support by the National Science Foundation (DMR-8704652), the donors of the Petroleum Research Fund, administered by the American Chemical Society, and the University of Oregon is also gratefully acknowledged.

Registry No. Mo, 7439-98-7; Se, 7782-49-2; $MoSe_2$, 12058-18-3.

(32) The interdiffusion process can be controlled by choosing the layering sequence of the modulation composite such that those elements that form very stable binary compounds do not have a change to interact directly. An example of this for ternary phases is the layering sequence Cu–Mo–Cu–Se instead of the layering sequence of Mo–Cu–Mo–Se. In the first example, the copper alloys almost immediately with the selenium and it is this compound that then interdiffuses with the molybdenum. In the second, the molybdenum and selenium alloy below the interdiffusion temperature of molybdenum and copper.

(33) Work in progress.

(34) Tung, R. T. *J. Vac. Sci. Technol. A* **1987**, *5*, 1840–1844.

(35) Glass ceramics are formed by the controlled crystallization of a glass such that many nuclei are formed. The resultant fine grained ceramics have very high strength and adjustable thermal expansion coefficients.

Ag(I) Modified Base Pairs Involving Complementary (G, C) and Noncomplementary (A, C) Nucleobases. On the Possible Structural Role of Aqua Ligands in Metal-Modified Nucleobase Pairs†

Stephan Menzer,[1a] Michal Sabat,*[1b] and Bernhard Lippert*[1a]

Contribution from the Fachbereich Chemie, Universität Dortmund, 4600 Dortmund, FRG, and Department of Chemistry, University of Virginia, Charlottesville, Virginia 22901.
Received November 18, 1991

Abstract: Two Ag(I) complexes containing the model nucleobases 1-methylcytosine (1-MeC), 9-methyladenine (9-MeA), and 7,9-dimethylguanine (7,9-DimeG) have been prepared and studied: $[Ag(1\text{-MeC-}N^3)(9\text{-MeA-}N^7)(H_2O)]NO_3$ (**2**) crystallizes in the space group $P2_1/a$, a = 11.167 (2) Å, b = 13.437 (2) Å, c = 11.520 (2) Å, β = 109.79 (2)°, V = 1626 (1) Å^3, Z = 4. Ag has a severely distorted trigonal-planar coordination geometry with two strong bonds (2.128 (2) Å and 2.120 (2) Å) to the nitrogens of the nucleobases and a weak bond (2.664 (2) Å) to a water molecule. The N–Ag–N vector is markedly nonlinear (angle at Ag 165.8 (1)°). Both nucleobases and the water molecule are virtually coplanar. Intramolecular H bonding is between O(2) of 1-MeC and N(6) of 9-MeA (3.053 (3) Å) as well as between N(4) of 1-MeC and the aqua ligand (2.894 (4) Å). Structural details of the structure of **2** clearly demonstrate that the water molecule is an integral part of the "metal-modified" base pair. A second mixed-nucleobase complex of composition $[Ag(1\text{-MeC})(7,9\text{-DimeG})NO_3]_2\cdot[(1\text{-MeC})(7,9\text{-DimeGH})PF_6]\cdot 10H_2O$ (**3**) has been prepared and characterized by elemental analysis and ^{1}H NMR spectroscopy. On the basis of the structure of **2** an alternative model to existing hypotheses on Ag–DNA interactions is put forward which considers the "insertion" of a metal-aqua entity into an existing base pair.

Introduction

Ever since interactions between metal ions and nucleic acids or their constituents, the nucleobases, became of general interest, Ag(I) has played a major role in such studies.[2-15] At an early stage it became evident, that Ag(I) has a distinct preference for binding to endocyclic ring nitrogen atoms, even with displacement of protons, e.g., N(3)H of thymine (uracil) and N(1)H of inosine.[7,11] Studies involving isolated nucleobases and models

† Dedicated to Prof. Wolfgang Beck.

(1) (a) University of Dortmund. (b) University of Virginia.

(2) Yamane, T.; Davidson, N. *Biochim. Biophys. Acta* **1962**, *55*, 609 and 780.

(3) Dove, W. F.; Davidson, N. *J. Mol. Biol.* **1962**, *5*, 467.

(4) Davidson, N.; Widholm, J.; Nandi, U. S.; Jensen, R.; Olivera, B. M.; Wang, J. C. *Proc. Natl. Acad. Sci. U.S.A.* **1965**, *53*, 111.

0002-7863/92/1514-4644$03.00/0